Fatty Acid Synthase Inhibition Activates AMP-Activated Protein Kinase in SKOV3 Human Ovarian Cancer Cells

Weibo Zhou,[1] Wan Fang Han,[1] Leslie E. Landree,[2] Jagan N. Thupari,[1] Michael L. Pinn,[1] Tsion Bililign,[6] Eun Kyoung Kim,[2] Aravinda Vadlamudi,[7] Susan M. Medghalchi,[7] Rajaa El Meskini,[7] Gabriele V. Ronnett,[2,3] Craig A. Townsend,[6] and Francis P. Kuhajda[1,4,5]

Departments of [1]Pathology, [2]Neuroscience, [3]Neurology, [4]Oncology, and [5]Biological Chemistry, The Johns Hopkins University School of Medicine; [6]Department of Chemistry, The Johns Hopkins University; and [7]FASgen, Inc., Baltimore, Maryland

Abstract

Fatty acid synthase (FAS), the enzyme responsible for the *de novo* synthesis of fatty acids, is highly expressed in ovarian cancers and most common human carcinomas. Inhibition of FAS and activation of AMP-activated protein kinase (AMPK) have been shown to be cytotoxic to human cancer cells *in vitro* and *in vivo*. In this report, we explore the cytotoxic mechanism of action of FAS inhibition and show that C93, a synthetic FAS inhibitor, increases the AMP/ATP ratio, activating AMPK in SKOV3 human ovarian cancer cells, which leads to cytotoxicity. As a physiologic consequence of AMPK activation, acetyl-CoA carboxylase (ACC), the rate-limiting enzyme of fatty acid synthesis, was phosphorylated and inhibited whereas glucose oxidation was increased. Despite these attempts to conserve energy, the AMP/ATP ratio increased with worsening cellular redox status. Pretreatment of SKOV3 cells with compound C, an AMPK inhibitor, substantially rescued the cells from C93 cytotoxicity, indicating its dependence on AMPK activation. 5-(Tetradecyloxy)-2-furoic acid, an ACC inhibitor, did not activate AMPK despite inhibiting fatty acid synthesis pathway activity and was not significantly cytotoxic to SKOV3 cells. This indicates that substrate accumulation from FAS inhibition triggering AMPK activation, not end-product depletion of fatty acids, is likely responsible for AMPK activation. C93 also exhibited significant antitumor activity and apoptosis against SKOV3 xenografts in athymic mice without significant weight loss or cytotoxicity to proliferating cellular compartments such as bone marrow, gastrointestinal tract, or skin. Thus, pharmacologic FAS inhibition selectively activates AMPK in ovarian cancer cells, inducing cytotoxicity while sparing most normal human tissues from the pleiotropic effects of AMPK activation. [Cancer Res 2007;67(7):2964–71]

Introduction

Although significant strides in the treatment and diagnosis of ovarian cancer have led to improved 5-year survival rates (1), ovarian cancer remains the leading cause of death from gynecologic cancers (2). Fatty acid synthase (FAS), the enzyme responsible for the *de novo* synthesis of fatty acids, has emerged as a potential therapeutic target for human cancer. FAS catalyzes the condensation of malonyl-CoA and acetyl-CoA to produce long-chain fatty acids (3). High levels of FAS expression have been found in ovarian cancer (4, 5) and in most human solid tumors (6). The up-regulation of FAS expression in cancer cells has been linked to both mitogen-activated protein kinase and phosphatidylinositol 3-kinase pathways through the sterol regulatory binding element binding protein 1c (7–9). FAS protein expression denotes poor prognosis in breast and prostate cancer (10–15) and is found elevated in the blood of cancer patients (16, 17). Inhibition of FAS activity is selectively cytotoxic to human cancer cells *in vitro* and *in vivo* (13, 18–21) including human ovarian cancer xenografts (20, 22).

The mechanism linking inhibition of FAS activity to cancer cell death remains an active area of investigation. Because endogenously synthesized fatty acids in cancer cells are incorporated predominantly into phospholipids (23), it was hypothesized that FAS inhibition reduced available fatty acids for structural lipid synthesis in these cells. However, FAS inhibition induced apoptosis whereas pharmacologic inhibition of acetyl-CoA carboxylase (ACC), the rate-limiting enzyme of fatty acid synthesis, was far less toxic and actually protected cancer cells from FAS inhibition (18, 24). These findings implicated the accumulation of FAS substrates such as malonyl-CoA, rather than the depletion of end-product fatty acids, as contributing to cancer cell death. In addition to fatty acid synthesis, a number of other pathways have been found to modulate cytotoxicity following FAS inhibition including p53 (25, 26), HER2/*neu* (27, 28), and Akt (20, 29). Whereas these pathways may alter the response of cancer cells to FAS inhibition, the link between FAS enzyme inhibition and cancer cell death remains elusive.

C75, a synthetic mammalian FAS inhibitor (30), provided much of the *in vivo* evidence of the selective antitumor activity of pharmacologic FAS inhibition (13, 18, 19). Treatment, however, was limited by anorexia and weight loss (18, 31). While investigating the mechanism of action of C75-induced weight loss, we discovered that, in addition to FAS inhibition, C75 also stimulated carnitine palmitoyltransferase-1 (CPT-1) activity, leading to substantially increased fatty acid oxidation (32–35). CPT-1 is the rate-limiting transporter of long-chain acyl-CoAs into the mitochondria for oxidation. These studies raised the possibility that increased fatty acid oxidation could be responsible for at least part of the anticancer effect of C75. However, *in vitro* studies of fatty acid oxidation (24) and short interfering FAS RNA treatment of cancer cells (21) have established that FAS is the target of C75-induced cytotoxicity in cancer.

Although FAS seems to be the target of C75 for cancer cytotoxicity, the mechanism involved in the induction of anorexia

Note: Under a licensing agreement between FASgen and the Johns Hopkins University, F.P. Kuhajda and C.A. Townsend are entitled to a share of royalty received by the University on sales of products described in this article. F.P. Kuhajda and C.A. Townsend own and G.V. Ronnett has an interest in FASgen stock, which is subject to certain restrictions under University policy. The Johns Hopkins University, in accordance with its conflict of interest policies, is managing the terms of this arrangement.

Requests for reprints: Francis P. Kuhajda, Department of Pathology, Johns Hopkins Bayview Medical Center, 4940 Eastern Avenue, Baltimore, MD 21224. Phone: 410-550-0671; Fax: 410-550-0075; E-mail: fkuhajda@jhmi.edu.

doi:10.1158/0008-5472.CAN-06-3439

involves the increase of fatty acid oxidation through CPT-1 stimulation, as well as the reduction of hypothalamic neuropeptide-Y expression (31). Further studies showed a pivotal role for AMP-activated protein kinase (AMPK) in the mechanism of C75-induced anorexia (36, 37). AMPK is activated in cells as a response to metabolic stresses that lead to the depletion of cellular ATP levels and thus the increase in AMP/ATP ratio (38, 39). The involvement of AMPK in the hypothalamic response to C75 (37) led to the hypothesis that the antitumor effect of FAS inhibition could also be mediated through changes in AMPK activation.

Thus, we and our collaborators sought to synthesize small-molecule FAS inhibitors that retain antitumor activity without inducing weight loss or stimulating fatty acid oxidation, which led to the development of C93 (40). In this study, we used human SKOV3 ovarian cancer cells to explore the role of AMPK in the cytotoxic mechanism of action of FAS inhibition using C93.

Materials and Methods

Cell lines, chemicals, and antibodies. SKOV3 human ovarian cancer cells, obtained from the American Type Culture Collection (Manassas, VA), were cultured in McCoy's 5A medium with 10% FCS and 1% penicillin/streptomycin. C93 and compound C were obtained from FASgen, Inc. (Baltimore. MD). 5-(Tetradecyloxy)-2-furoic acid (TOFA) was synthesized by C.A. Townsend (Department of Chemistry, Johns Hopkins University, Baltimore, MD). C93, compound C, and TOFA were added to the cultures from 5 mg/mL stock solutions in 100% DMSO to give the indicated concentrations and the final DMSO concentration in cultures was ≤0.2%. Antibodies to pACC, pAMPK, AMPK, and β-actin were obtained from Cell Signaling (Danvers, MA). Mouse monoclonal antibodies to human FAS were obtained courtesy of FASgen.

To generate AMPK isoform–specific antibodies, rabbits were immunized with a peptide corresponding to amino acids 339 to 358 (DFY-LATSPPDSFLDDHHLTR) of rat AMPKα1 or amino acids 352 to 366 (MDDSAMHIPPGLKPH) of α2 (41, 42). The keyhole limpet hemocyanin/GGG–conjugated peptides were injected to produce antibodies. The peptide-specific affinity-purified antibodies were used for SAMS peptide AMPK activity assay.

Cell viability assay. To measure the cytotoxicity of specific compounds against cancer cells, 9×10^3 SKOV3 cells were plated per well onto 96-well plates. Following overnight culture, the compounds, dissolved in 100% DMSO, were added to the wells in 1-μL volume at specified concentrations. Vehicle controls were run for each experiment. Each condition was run in triplicate.

After 24 or 72 h of incubation, cells were incubated for 4 h with the 2,3-bis[2-methoxy-4-nitro-5-sulfophenyl]-2*H*-tetrazolium-5-carboxanilide inner salt (XTT) reagent as per manufacturer's instructions (Cell Proliferation Kit II, Roche Diagnostics, Indianapolis, IN). Plates were read at A_{490} and A_{650} on a SpectraMax Plus Spectrophotometer (Molecular Devices, Sunnyvale, CA). Three wells containing the XTT reagent without cells served as the plate blank. XTT data were reported as $A_{490} - A_{650}$. Averages and SEs were computed using SOFTmax Pro software (Molecular Devices). The LC_{50} for each compound was defined as the concentration of drug leading to a 50% reduction in $A_{490} - A_{650}$ compared with controls. LC_{50} was calculated by linear regression, plotting the FAS activity as percent of control versus drug concentrations. Linear regression, best-fit line, r^2, and 95% confidence intervals were determined using GraphPad Prism version 4.0 (GraphPad Software, San Diego, CA).

Purification and assay of rat FAS. Frozen livers from rats induced for FAS production were obtained from Pel-Freeze Biologicals (Rogers, AR). Purification of FAS was adopted from Smith and Abraham (43) with minor modifications. An analogous protocol was used to isolate the human enzyme from a cultured ZR-75-1 breast cancer cell line provided by FASgen.

The specific activity and steady-state kinetic constants for overall FAS activity were similar to those reported in the literature for the rat (44) and human (45) enzyme. Overall FAS activity was monitored spectrophotometrically by following the oxidation of NADPH at 240 nm [ε = 6,220 $(mol/L)^{-1}$ cm^{-1}] in the presence of the physiologic substrates malonyl-CoA and acetyl-CoA, as previously reported (43). Inhibition was monitored by varying concentrations of test compound in the overall FAS assay and IC_{50} values were determined by regression analysis (sigmoidal dose response) of the inhibition data (SigmaPlot, Point Richmond, CA).

Fatty acid synthesis. Fatty acid synthesis was measured by incorporation of [U-^{14}C]acetate into lipids as described (18). Briefly, SKOV3 cells were cultured in 24-well plates at 5×10^4 per well and incubated overnight. After the addition of drugs or vehicle alone as indicated, cells were pulse labeled with [U-^{14}C]acetate, 1 μCi/well for 30 min to 2 h. Each condition was run in triplicate. Lipids were Folch extracted, counted for ^{14}C, and data were expressed as percent of control.

Fatty acid oxidation. Fatty acid oxidation was measured by isolation of acid soluble products as described (46). Briefly, 2.5×10^5 cells were plated onto 24-well plates. Following overnight culture, cells were incubated with drug for 60 min at 37°C for specified doses. The medium was removed and 250 μL of reaction buffer [100 μmol/L [U-^{14}C]palmitate (1.42 μCi), 200 μmol/L carnitine in serum-free medium with appropriate concentration of drug] were added for 30 min. The reaction was stopped with 50 μL of 2.6 N $HClO_4$ and neutralized with 50 μL of 4 N KOH. Cells were incubated at 60°C for 30 min and 75 μL of 1 mol/L sodium acetate and 50 μL of 3 N H_2SO_4 were added. Cells were centrifuged at $1,000 \times g$ for 7 min and extracted with 1:1 chloroform/methanol. The aqueous phase was counted for ^{14}C. Each condition was run in triplicate; data were expressed as percent of control.

Glucose oxidation. Glucose oxidation was measured in SKOV3 cells as described (47). Briefly, 10^6 adherent SKOV3 cells were treated with C93 in Krebs-Ringer bicarbonate HEPES buffer containing 1% bovine serum albumin and 5 mmol/L glucose (47) at concentrations and times indicated. For the final 30 min of each treatment, 0.5 μCi/mL [U-^{14}C]glucose was added. Reactions were stopped with 7% $HClO_4$, and 400 μL of benzethonium hydroxide were injected in the center well. After 2 h at 37°C, complete oxidation was quantified by measuring the amount of ^{14}C in the center well by liquid scintillation counting. Each condition was run in triplicate; data were expressed as percent of control.

Western blot analysis. Cells were homogenized in lysis buffer consisting of 50 mmol/L Tris-HCl (pH 7.5), 250 mmol/L sucrose, 5 mmol/L sodium pyrophosphate, 50 mmol/L NaF, 1 mmol/L EDTA, 1 mmol/L EGTA, 1 mmol/L DTT, 0.5 mmol/L benzamidine, 50 μg/mL leupeptin, and 50 μg/mL soybean trypsin inhibitor. SDS was added to a concentration of 0.2% and proteins were separated on 4% to 15% polyacrylamide gradient gels and transferred to a polyvinylidine difluoride membrane. Blots were probed with anti-pAMPK, anti-AMPK, anti-FAS, or anti–β-actin. Samples for pACC immunoblots were run on separate 5% polyacrylamide gels.

Measurement of adenine and pyridine nucleotides. Both adenine and pyridine nucleotides (ATP, ADP, AMP, NAD^+, NADH, $NADP^+$, and NADPH) were measured concomitantly using high-performance liquid chromatography as described (48). Briefly, 1×10^6 SKOV3 cells were plated onto 60-mm dishes and treated as described. Pyridine and adenine nucleotides were extracted with alkali before high-performance liquid chromatography analysis. Cell extracts and purified nucleotide controls (Sigma) were separated and quantified using an Agilent 1100 running ChemStation software as follows: 50 μL of the supernatants were loaded onto an LC-18 column and absorbance at 254 nm was measured. The two eluants were buffer A: 0.1 mol/L KH_2PO_4, 8 mmol/L tetrabutylammonium hydrogen sulfate, pH 6.0; and buffer B: 70% buffer A in methanol. The following gradients were carried out: 0 to 2.5 min, 100% A; 2.5 to 5.0 min, 80% A; 5.0 to 10.0 min, 60% A: 10.0 to 13.0 min, 0% A (100% B), for 5 min. The flow rate was 1.5 mL/min. Data were expressed as ratios of redox couples or as absorbance at 254 nm.

Measurement of AMPK activity. AMPK activity was measured by carrying out the SAMS peptide assay as described (36, 49). SKOV3 cells were plated onto six-well dishes and three wells were used per condition. AMPKα1 or AMPKα2 isoforms were immunoprecipitated in the presence of isoform-specific antibodies coupled to protein A/G beads (Santa Cruz

Biotechnology, Santa Cruz, CA). Immunoprecipitates were washed and kinase activity was assessed by incorporation of ^{32}P into the synthetic SAMS peptide substrate (Princeton Biomolecules, Langhorne, PA). Each sample was corrected for protein concentration and triplicate assays were reported as percent of control.

Animal studies. All animal experiments were done in accordance with guidelines on animal care and use established by the Johns Hopkins University School of Medicine Institutional Animal Care and Use Committee. Female athymic nude BALB/c mice (8–10 weeks) were purchased from Harlan Laboratories (Indianapolis, IN) and housed in a pathogen-free facility. Animals were treated once or twice daily with i.p. injections of C93, with 50 mg/kg dissolved in 50 μL of 100% DMSO, or with vehicle alone as specified. For i.p. xenografts, 5×10^7 SKOV3 cells were injected. After seven days, C93 was administered i.p. at 50 mg/kg daily in DMSO every fifth day for 4 weeks. Wet tumor weight was obtained at necropsy. For flank xenografts, 2×10^6 SKOV3 cells were injected and treatment commenced when tumors reached 100 mm^3. C93 was administered i.p. at 50 mg/kg twice a day in 100% DMSO on each day except days 6 and 13. Tumor volume and animal weights were measured daily.

Results

C93 inhibits FAS and is cytotoxic to SKOV3 cells but does not increase fatty acid oxidation or induce weight loss. C93 emerged from a screen of potential inhibitors assayed against homogenous FAS isolated from rat liver and ZR-75-1 human breast cancer cells. The development of C93 accomplished the pharmacologic elimination of CPT-1 stimulation while preserving FAS inhibition. Thus, C93 does not substantially affect weight loss or feeding behavior as seen with C75 (40, 50). Highlighted in Table 1 are key features of C93 compared with C75 and TOFA, an inhibitor of ACC (51). Both C93 and C75 inhibit FAS, but C93 is 2-fold more effective in pathway inhibition and >3-fold more toxic to SKOV3 cells. Importantly, C93 does not stimulate CPT-1 or increase fatty acid oxidation as does C75. As a result, C93 induced a 1.4% weight loss in lean BALB/c mice with a single i.p. 60 mg/kg dose, compared with a 15% weight loss with a single i.p. 30 mg/kg dose of C75. Similar to our previous report (18), ACC inhibition with TOFA was less cytotoxic than FAS inhibition. TOFA, although >25-fold more effective in pathway inhibition than C93 in SKOV3 cells, was 16-fold less effective as a cytotoxic agent against SKOV3 cells compared with C93. Thus, inhibition of the fatty acid synthesis pathway by FAS is substantially more efficacious compared with inhibition by the physiologic rate-limiting enzyme ACC.

C93 rapidly inhibits fatty acid synthesis and activates AMPK. To establish the time course of events following C93 treatment of SKOV3 cells, we first determined how rapidly C93 inhibited fatty acid synthesis by measuring the incorporation of [^{14}C]acetate into lipids (Fig. 1*A*). Initially, C93 inhibited fatty acid synthesis pathway activity by ~60% relative to vehicle control by 30 min posttreatment. By 160 min posttreatment, fatty acid synthesis activity decreased to 40% of the control. We next measured ATP and AMP levels to assess cellular energy status over the same time course. Using the same concentrations of C93 and culture conditions, a significant elevation in the AMP/ATP ratio occurred within 30 min of C93 treatment (Fig. 1*B*). The AMP/ATP ratio continued to increase to >2-fold compared with control at 180 min posttreatment. Concomitant with the increase in the AMP/ATP ratio, C93 treatment enhanced AMPK phosphorylation detected by immunoblot within 30 min of treatment persisting through 180 min (Fig. 1*C*). AMPK phosphorylation was accompanied by phosphorylation of one of its target proteins, ACC, detected 120 min posttreatment. The activation of AMPK has been shown to phosphorylate and inhibit ACC, thus reducing fatty acid synthesis pathway activity, thereby preserving ATP (52). Thus, ACC phosphorylation may be responsible for the continued reduction in FAS pathway activity at 160 min post C93 treatment seen in Fig. 1*A*. Recently, AMPK activation has been reported to reduce FAS expression (53). Whereas changes in FAS expression would be unlikely to account for the rapid reduction in pathway activity, nonetheless, an immunoblot showed no change in FAS protein expression compared with the β-actin control during the course of C93 treatment (Fig. 1*C*).

Increased AMPK phosphorylation denotes increased AMPK activity. To confirm the biological significance of the AMPK phosphorylation and directly measure AMPK activity, SAMS peptide activity assays were done (Fig. 1*D*). In the inset, immunoblots of SKOV3 cells showed predominance of the α2 isoform over the α1 isoform. Using antibodies selective for the α2 isoform, an ~150% increase in AMPK activity was noted at 30 min following C93 treatment, which continued to increase to >200% of control by 120 min posttreatment. Taken together, these data strongly suggest that C93 treatment rapidly activates AMPK in SKOV3 cells.

C93 increases glucose oxidation while reducing both NAD^+/NADH and $NADP^+$/NADPH ratios. Whereas AMPK activation reduces the activity of anabolic pathways to preserve energy expenditure, it concomitantly increases the activity of catabolic pathways in an attempt to replenish ATP levels. Figure 2*A* shows that following C93 treatment, SKOV3 cells significantly increased glucose oxidation compared with controls within 60 min of treatment. However, despite the increased glucose oxidation noted at 60 min posttreatment, the AMP/ATP ratio did not improve (Fig. 1*B*). In addition to the increasing AMP/ATP ratio, Fig. 2*B*

Table 1. Comparison of C93, C75, and TOFA

Drug	Target	FAS inhibition IC_{50} (μg/mL)	Pathway inhibition IC_{50} (μg/mL)	SKOV3 XTT LC_{50} (μg/mL)	CPT-1 stimulation	FAO stimulation SC_{150} (μg/mL)	Maximum weight loss [% (i.p. dose)]
C93	FAS	30	5.5 ± 0.5	2.6 ± 0.3	None	None	1.4 (60 mg/kg)
C75	FAS/CPT-1	10	10.8 ± 2.7	11.0 ± 2.3	300% at 20 μg/mL	1.7 ± 2.0	15.0 (30 mg/kg)
TOFA	ACC	NA	0.20 ± 0.024	42.4 ± 1.8	None	None	0 (60 mg/kg)

Abbreviations: FAO, fatty acid oxidation; SC_{150}, stimulatory concentration 150; NA, not applicable.

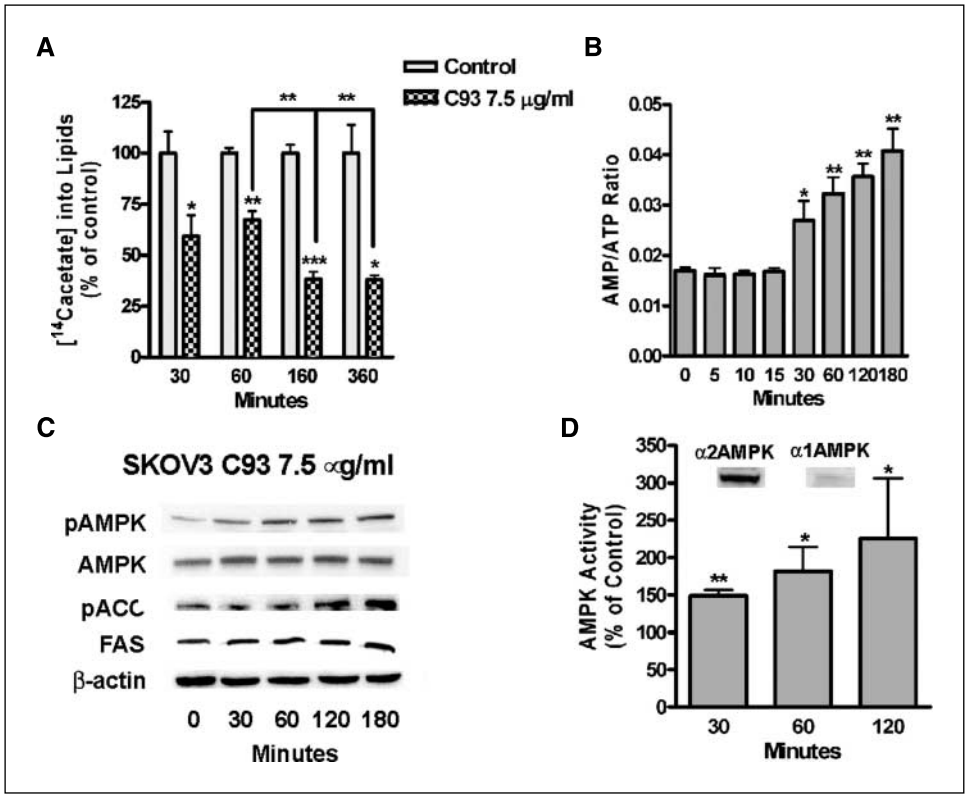

Figure 1. C93 inhibits fatty acid synthesis and increases the AMP/ATP ratio, activating AMPK in SKOV3 cells. *A,* C93 inhibited fatty acid synthesis within 30 min of treatment with further inhibition occurring 160 min posttreatment (two-tailed *t* tests). *B,* the AMP/ATP ratio increased within 30 min following C93 treatment ($P < 0.0001$). The overall *P* value was calculated by one-way ANOVA analysis; *P* values for all individual time points were calculated with time 0 as the control value using Dunnett's posttest. *C,* immunoblot showing AMPK and ACC phosphorylation 30 and 120 min following C93, respectively. There was no change in FAS expression. *D,* following C93 treatment, AMPK activity, as measured by SAMS peptide assay, increased as compared with vehicle control (two-tailed *t* tests). AMPK activity paralleled AMPK phosphorylation as shown in (*C*). Immunoblots showed that SKOV3 cells predominantly express the α2 AMPK isoform (*insets*; *, $P < 0.05$; **, $P < 0.01$; ***, $P < 0.001$; GraphPad Software).

shows that following C93 treatment, the NAD^+/NADH ratio declined, indicating a failure of the cell to maintain a positive redox balance.

FAS uses the reductive power of NADPH in the synthesis of fatty acids with the oxidation of 14 mol of NADPH per mole of fatty acid synthesized. Thus, inhibition of FAS might be expected to increase, at least transiently, NADPH levels. Figure 2*C* shows that NADPH levels indeed increased within 5 min following C93 treatment without a substantial change in the NADPH/$NADP^+$ ratio (Fig. 2*D*). After 60 min, however, the NADPH/$NADP^+$ ratio begins to decline, which may reflect the overall waning in reductive biosynthesis activity that follows AMPK activation (52).

Compound C rescues C93-induced cytotoxicity. If AMPK activation contributes to C93 cytotoxicity, blocking AMPK activation with compound C, an AMPK inhibitor (37, 54), should blunt the cytotoxic effect of C93 treatment. Figure 3*A* represents three separate experiments in which SKOV3 cells were treated with C93 alone, C93 combined with a 1-hour pretreatment with compound C, or compound C alone. Compound C pretreatment substantially reduced the cytotoxicity of C93 assayed 24 h post-treatment. Treatment with compound C alone at the same concentration had no significant cytotoxic effect on SKOV3 cells. These data suggest that AMPK activation plays a substantial role in the cytotoxic mechanism of action of C93.

TOFA does not activate AMPK and is not toxic to SKOV3 cells at a concentration that substantially inhibits fatty acid synthesis. Because ACC inhibition has been shown to be less cytotoxic to human cancer cells than inhibition of fatty acid synthesis at FAS (18), we hypothesized that TOFA treatment would not increase AMPK phosphorylation. In Fig. 3*B*, TOFA treatment at 5 μg/mL, a concentration that dramatically reduced fatty acid synthesis (Table 1), did not substantially affect AMPK phosphorylation. In contrast, 5-aminoimidazole-4-carboxamide-1-β-D-ribofuranoside (AICAR), an activator of AMPK, caused substantial AMPK phosphorylation in SKOV3 cells at 1 mmol/L (Fig. 3*B, lane A*).

Because TOFA does not activate AMPK, we next compared TOFA with C93 and AICAR in a cytotoxicity assay (Fig. 3*C*). After 24 h, C93 reduced the viability of SKOV3 cells to 75% of vehicle control, whereas TOFA, at a concentration that substantially inhibits fatty acid synthesis pathway activity, did not significantly affect cell viability. AICAR, an activator of AMPK, was also substantially cytotoxic. Thus, C93 and AICAR, which both activate AMPK, were cytotoxic to SKOV3 cells, whereas TOFA was not. These data further substantiate that (*a*) AMPK activation is cytotoxic to human cancer cells (55); (*b*) inhibition of ACC with TOFA does not lead to increased AMPK phosphorylation, consistent with previous experiments using cultured neurons (36); and (*c*) inhibition of fatty acid synthesis does not activate AMPK.

C93 inhibits the growth of the SKOV3 xenograft. Whereas C93 is effective as a cytotoxic agent against SKOV3 cells *in vitro*, we did a pilot studies of C93 to asses the antitumor activity of C93 in SKOV3 xenograft–bearing mice. In the SKOV3 i.p. xenograft model (ref. 20; Fig. 4*A*), the five informative C93-treated animals had an average tumor volume of ~14 g compared with 110 g for the vehicle controls. Three of the treated animals had no identifiable residual tumor. No significant weight loss was identified. There were peritoneal adhesions in the C93-treated animals bearing i.p. xenografts. In this group, three animals were lost due to gastrointestinal trauma during i.p. injections.

Figure 4*B* illustrates the antitumor effect of C93 on a s.c. xenograft of SKOV3 cells in athymic mice. C93 inhibited tumor growth 3-fold compared with vehicle controls ($P < 0.0001$, repeated measures two-way ANOVA analysis; GraphPad Prism version 4.00 for Windows). At

the conclusion of the study, the control animals weighed 97.5 ± 1.2% of pretreatment weight compared with 95.0% ± 2.5% for the C93-treated animals (not significant; $P > 0.050$, two-tailed t test). Thus, nonoptimized treatment of the SKOV3 xenograft with C93 produced a significant antitumor response without significant weight loss. Histopathologic analysis of C93 SKOV3 xenografts showed extensive tumor cytotoxicity characterized by acute inflammation (Fig. 4*C, arrows*) compared with vehicle control (Fig. 4*D*). Necropsy of the animals at the conclusion of both studies showed no gross or microscopic evidence of cytotoxicity to proliferating cell compartments including skin, gastrointestinal tract, or bone marrow (data not shown).

Discussion

With the extensive array of human cancers that express high levels of FAS and the numerous studies documenting the cytotoxic effects of FAS inhibition both *in vitro* and *in vivo* (6), FAS holds promise as a new drug target for cancer therapy. Whereas our initial studies with C75, a synthetic FAS inhibitor (30), showed significant antitumor activity against human xenografts, treatment was limited by dramatic weight loss (18, 31, 56). We and our collaborators sought to understand the mechanism responsible for C75-induced weight loss to determine if it was (*a*) common to all FAS inhibitors, (*b*) unique to C75, (*c*) due to action at a second drug target, or (*d*) the result of nonspecific sickness behavior. It now seems that C75-induced weight loss occurred predominantly from increased fatty acid oxidation via stimulation of CPT-1, rather than solely through FAS inhibition (57). The pharmacologic separation of CPT-1 stimulation from FAS inhibition led to the development of C93, which affords substantial anticancer cytotoxicity *in vitro* and *in vivo* without the weight loss seen with C75 treatment.

C93 also allowed the further pursuit of the cytotoxic mechanism of action of FAS inhibition. The involvement of AMPK in the hypothalamic response to C75 (37) and studies linking AMPK activation to cell cycle arrest in transformed cells (55) led us to hypothesize that AMPK may be involved in the cytotoxic response of FAS inhibition. AMPK is a heterotrimeric complex consisting of catalytic subunit α1 or α2 and regulatory β and γ subunits, which function as a serine/threonine kinase (58). Once activated by phosphorylation, AMPK inactivates anabolic biosynthetic enzymes for cholesterol synthesis, such as hydroxymethylglutaryl-CoA reductase, and for fatty synthesis, such as ACC, curbing ATP utilization (38, 52). Concomitantly, AMPK stimulates catabolic processes that enhance ATP production such as glucose uptake, glycolysis, and fatty acid oxidation (59–62).

AMPK itself has been proposed as a therapeutic target for cancer (55, 63, 64). AMPK activation has been shown to induce cell cycle arrest in transformed cell lines such as HepG2 (55, 65) and in nontransformed vascular smooth muscle cells (66). In a recent study, AICAR treatment reduced cell proliferation in a number of cancer cell lines *in vitro* including C_6 rat transformed glioma, MCF-7 human breast, and PC3 human prostate (55). AICAR produced an S-phase arrest likely mediated by p21, p27, and p53 proteins and inhibition of Akt activation. *In vivo* treatment of C_6 glioma cells in rats with AICAR reduced tumor mass and cell proliferation. Importantly, AICAR inhibited proliferation of $LKB^{-/-}$ mouse embryo fibroblasts showing independence of the *LKB*

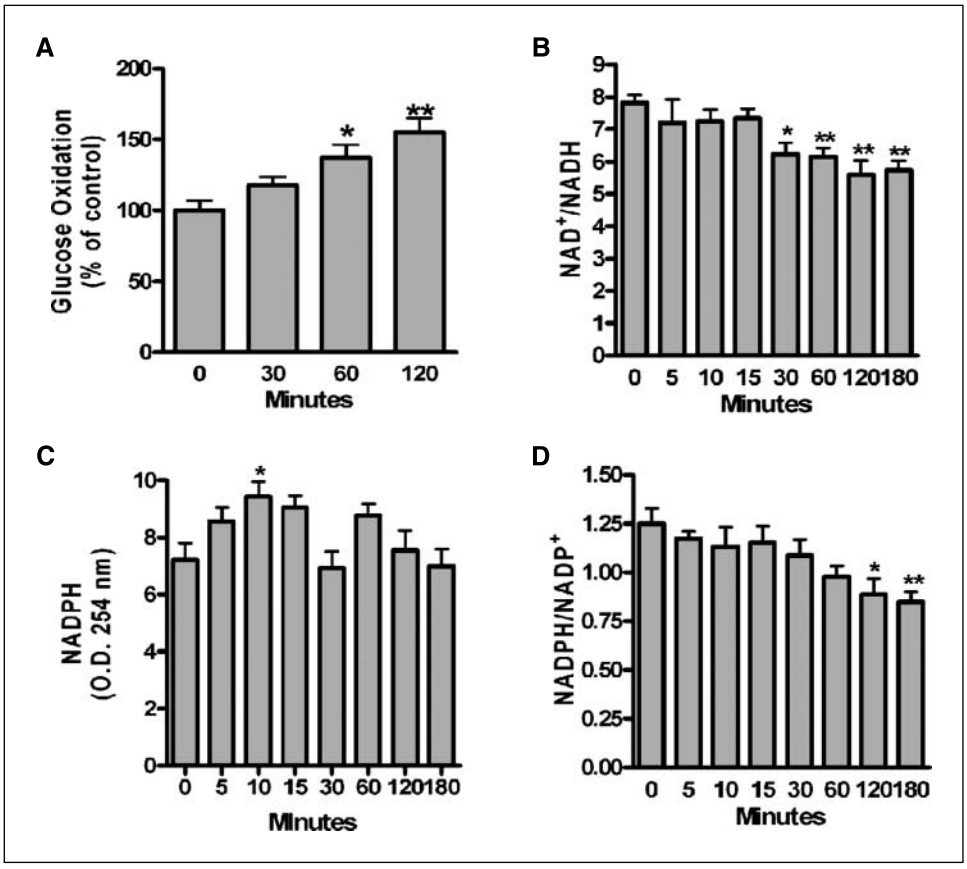

Figure 2. C93 increased glucose oxidation and altered redox balance in SKOV3 cells. *A,* glucose oxidation was increased within 60 min of C93 treatment ($P = 0.0009$). *B,* despite increased glucose oxidation, the NAD^+/NADH redox couple declined ($P < 0.0001$). *C,* NADPH levels increased 5 min after C93 treatment but began to decline after 2 h ($P = 0.008$). *D,* the NADPH/$NADP^+$ redox couple was reduced 2 h after C93 treatment ($P = 0.013$). *P* values were calculated using one-way ANOVA analysis; *P* values for all individual time points were calculated with time 0 as the control value using Dunnett's posttest (*, $P < 0.05$; **, $P < 0.01$; ***, $P < 0.001$; Prism 4.0, GraphPad Software).

cancer suppressor gene (55). Whereas these studies indicate a link between cancer cell growth and the status of AMPK activation, nonselective activation of AMPK in the whole organism may not be suitable for therapy due to the pleiotropic effects of AMPK activation (67).

FAS inhibition was first linked to AMPK activation through studies with C75 in neurons and the central nervous system (36, 37). In primary cultures of cortical neurons, C75 and cerulenin, a natural product FAS inhibitor (68), initially activated AMPK within minutes followed by inactivation over hours with no evidence of cellular injury. In addition, ACC inhibition with TOFA failed to show a change in AMPK activation (36). In the hypothalamus, C75 rapidly inactivated AMPK, leading to anorexia. AICAR reversed the effect of AMPK whereas compound C, an AMPK inhibitor, mimicked the effect of C75 (37). Thus, feeding behavior, FAS activity, and AMPK activation were involved in the hypothalamic control of food intake. Because C75 was shown to inhibit the growth of human cancer cells, we hypothesized that AMPK may also be involved in the cytotoxic effect of FAS inhibition on cancer cells (13, 18–21).

The increased NADPH levels following C93 treatment suggests that significant inhibition of FAS occurs within minutes of treatment. We detected significant inhibition of the fatty acid synthesis pathway within 30 min of C93 treatment with the lag time likely due to the limitations of [^{14}C]acetate metabolic labeling of lipids. FAS inhibition was followed by a significant reduction in the AMP/ATP ratio also within 30 min of treatment. If an increase in the AMP/ATP ratio is biologically significant enough to signal an energy poor state, it should also activate AMPK through phosphorylation. Both by immunoblot and SAMS peptide assay, AMPK was activated within 30 min following C93 treatment. Thus, C93 rapidly inhibited FAS and induced an energy-poor state in the cancer cells with activated AMPK.

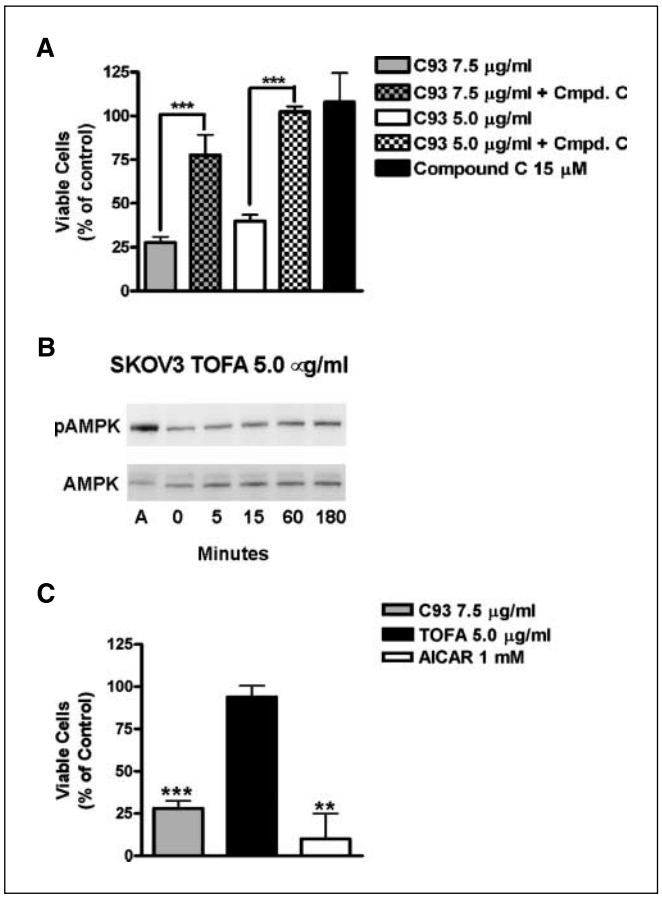

Figure 3. Compound C, an AMPK inhibitor, rescued SKOV3 cells from C93 cytotoxicity; TOFA, an ACC inhibitor, did not activate AMPK. *A,* SKOV3 cells pretreated with compound C were not susceptible to C93-induced cytotoxicity. *B,* immunoblot showed that treatment of SKOV3 cells with TOFA did not activate AMPK. *C,* both C93 and AICAR, AMPK activators, were significantly cytotoxic whereas TOFA failed to induce significant cytotoxicity compared with vehicle-treated controls (two-tailed *t* tests: *, $P < 0.05$; **, $P < 0.01$; ***, $P < 0.001$; Prism 4.0, GraphPad Software).

If the downstream signal transduction pathways are intact in SKOV3 cells, AMPK activation should reduce anabolic pathways and enhance catabolism. Two hours after C93 treatment, ACC was phosphorylated and fatty acid synthesis was further reduced, likely representing inhibition of ACC activity due to its phosphorylation. Within 60 min posttreatment, glucose oxidation was significantly increased. Thus, AMPK activation phosphorylated and inhibited ACC to reduce fatty acid synthesis while increasing catabolic glucose oxidation. Interestingly, AMPK activation has been shown to suppress FAS expression in primary cultured hepatocytes (53) and in androgen-independent (DU145 and PC3) and androgen-sensitive (LNCaP) cells (64). Whereas chronic AMPK activation may change the phenotype of cancer cells including FAS expression, it is unlikely that the rapidity of the changes following C93 treatment could be explained by reduced FAS expression because the half-life of the enzyme in cancer cells is ~12 h (data not shown). Indeed, over the course of these experiments, no changes in the FAS expression were identified by immunoblot.

Although the increased AMP/ATP ratio following C93 treatment activated AMPK and increased glucose oxidation, the AMP/ATP ratio continued to increase. Moreover, the oxidative potential of the cells reflected in the NAD^+/NADH ratio declined steadily 30 min posttreatment. Thus, although glucose oxidation increased, it was unable to compensate for the loss of ATP. The declining NAD^+/NADH ratio indicated a diminished capacity to further increase catabolism in response to the increasing AMP/ATP ratio. The anabolic redox couple $NADP^+$/NADPH was also substantially affected by C93 treatment. Within 10 min of treatment, NADPH levels were significantly elevated, perhaps reflecting the rapid inhibition of FAS leading to substrate accumulation. By 60 min, however, the NADPH/$NADP^+$ ratio began decreasing, which could impede macromolecular synthesis. Indeed, potent inhibition of DNA replication and S-phase progression in human cancer cells was noted with both cerulenin and C75 treatment (24, 25).

If AMPK activation is responsible for triggering cytotoxicity, prior treatment with compound C to block AMPK activation should blunt the cytotoxic effect of FAS inhibition. Indeed, pretreatment with compound C substantially rescued SKOV3 cells from C93 treatment. AMPK inactivation with compound C had no significant cytotoxic effect on SKOV3 cells. These data implicate AMPK activation in the cytotoxic mechanism of action of pharmacologic FAS inhibition with C93.

Prior studies from our laboratory with human breast cancer cells showed that FAS inhibition was substantially more cytotoxic than ACC inhibition (18). These data suggested that substrate accumulation, not end-product (fatty acid) depletion, was responsible for the cytotoxicity. In SKOV3 cells, although the IC_{50} for pathway inhibition with TOFA was >25-fold less than C93, the TOFA LC_{50} for SKOV3 cells was 16-fold greater. Moreover, TOFA treatment did not lead to AMPK phosphorylation. C93 and AICAR, both AMPK

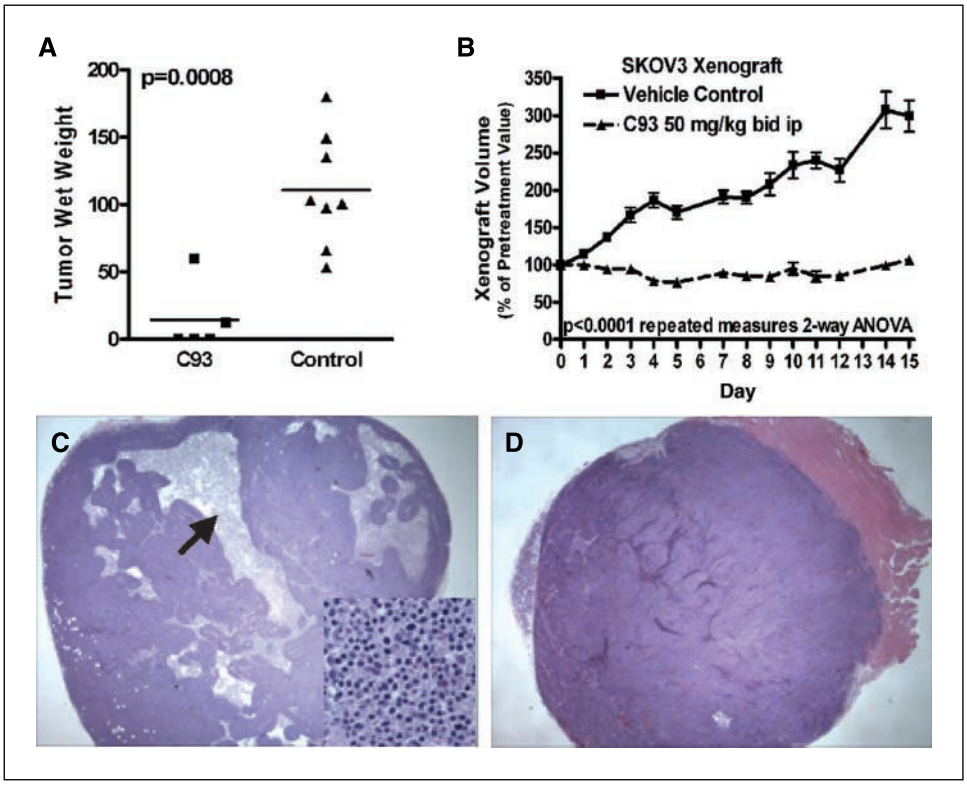

Figure 4. C93 inhibited the growth of SKOV3 xenografts. *A,* i.p. C93 treatment of an i.p. SKOV3 xenograft (n = 8) showed significant reduction in tumor volume with three animals tumor-free (two-tailed t test; GraphPad Software). Three C93-treated animals died from traumatic i.p. injections. *B,* to assess systemic C93 efficacy, s.c. SKOV3 xenografts were treated with i.p. C93. There was substantial reduction in tumor growth (repeated measures two-way ANOVA; Prism 4.0 GraphPad Software). *C,* xenograft treated with C93. Note the geographic areas of intense intratumoral acute inflammation and tumor cytotoxicity (*arrows*; ×200), which are absent from the vehicle control (*D*; ×200; H&E staining).

activators, were substantially cytotoxic to SKOV3 cells after 24 h, with no cytotoxicity detected with TOFA.

To determine the efficacy and any potential toxicity of C93 *in vivo*, we treated i.p. and s.c. SKOV3 xenograft–bearing athymic mice with C93 in two pilot studies. In the i.p. SKOV3 xenograft model (20), C93 daily i.p. treatment (50 mg/kg) substantially reduced tumor growth compared with vehicle controls with no identifiable disease in three animals. We next studied s.c. SKOV3 xenografts, escalating the dose to twice-daily C93 treatment for 2 weeks. The C93-treated mice had a 3-fold reduction in tumor growth compared with vehicle controls. Histopathology of the xenograft 4 h after treatment showed evidence of ongoing cytotoxicity characterized by foci of acute inflammation. No cytotoxic effect on other proliferating cell compartments such as skin, gastrointestinal tract, or bone marrow was noted.

The pharmacologic inhibition of FAS with C93 causes rapid energy depletion, AMPK activation, and substantial cytotoxicity *in vitro*. Pilot studies in the SKOV3 xenograft showed significant antitumor effect without evidence of significant toxicity or weight loss. Because FAS is up-regulated in cancer cells but not in normal human tissues (69), pharmacologic FAS inhibition may provide a means to selectively activate AMPK and induce a cytotoxic response in ovarian cancer while sparing most of normal human tissues from the pleiotropic effects of AMPK activation.

Acknowledgments

Received 9/25/2006; revised 12/13/2006; accepted 1/17/2007.

Grant support: NIH grants CA87850 (F.P. Kuhajda), Small Business Innovation Research National Cancer Institute grant 1R44CA99435 (to FASgen), and FASgen.

The costs of publication of this article were defrayed in part by the payment of page charges. This article must therefore be hereby marked *advertisement* in accordance with 18 U.S.C. Section 1734 solely to indicate this fact.

References

1. Armstrong DK. Relapsed ovarian cancer: challenges and management strategies for a chronic disease. Oncologist 2002;7 Suppl 5:20–8.
2. Bhoola S, Hoskins WJ. Diagnosis and management of epithelial ovarian cancer. Obstet Gynecol 2006;107: 1399–410.
3. Wakil S. Fatty acid synthase, a proficient multifunctional enzyme. Biochemistry 1989;28:4523–30.
4. Alo PL, Visca P, Framarino ML, et al. Immunohistochemical study of fatty acid synthase in ovarian neoplasms. Oncol Rep 2000;7:1383–8.
5. Gansler TS, Hardman W III, Hunt DA, Schaffel S, Hennigar RA. Increased expression of fatty acid synthase (OA-519) in ovarian neoplasms predicts shorter survival. Hum Pathol 1997;28:686–92.
6. Kuhajda FP. Fatty acid synthase and cancer: new application of an old pathway. Cancer Res 2006;66: 5977–80.
7. Yang YA, Han WF, Morin PJ, Chrest FJ, Pizer ES. Activation of fatty acid synthesis during neoplastic transformation: role of mitogen-activated protein kinase and phosphatidylinositol 3-kinase. Exp Cell Res 2002; 279:80–90.
8. Yang YA, Morin PJ, Han WF, et al. Regulation of fatty acid synthase expression in breast cancer by sterol regulatory element binding protein-1c. Exp Cell Res 2003;282:132–7.
9. Van de Sande T, De Schrijver E, Heyns W, Verhoeven G, Swinnen JV. Role of the phosphatidylinositol 3′-kinase/PTEN/Akt kinase pathway in the overexpression of fatty acid synthase in LNCaP prostate cancer cells. Cancer Res 2002;62:642–6.
10. Bull JH, Ellison G, Patel A, et al. Identification of potential diagnostic markers of prostate cancer and prostatic intraepithelial neoplasia using cDNA microarray. Br J Cancer 2001;84:1512–9.
11. Swinnen JV, Roskams T, Joniau S, et al. Overexpression of fatty acid synthase is an early and common event in the development of prostate cancer. Int J Cancer 2002;98:19–22.
12. Epstein JI, Carmichael M, Partin AW. OA-519 (fatty acid synthase) as an independent predictor of pathologic state in adenocarcinoma of the prostate. Urology 1995;45:81–6.
13. Pizer ES, Pflug BR, Bova GS, Han WF, Udan MS, Nelson JB. Increased fatty acid synthase as a therapeutic target in androgen-independent prostate cancer progression. Prostate 2001;47:102–10.
14. Alo PL, Visca P, Marci A, Mangoni A, Botti C, Di

Tondo U. Expression of fatty acid synthase (FAS) as a predictor of recurrence in stage I breast carcinoma patients. Cancer 1996;77:474–82.
15. Milgraum LZ, Witters LA, Pasternack GR, Kuhajda FP. Enzymes of the fatty acid synthesis pathway are highly expressed in *in situ* breast carcinoma. Clin Cancer Res 1997;3:2115–20.
16. Wang Y, Kuhajda FP, Sokoll LJ, Chan DW. Two-site ELISA for the quantitative determination of fatty acid synthase. Clin Chim Acta 2001;304:107–15.
17. Wang YY, Kuhajda FP, Cheng P, et al. A new model ELISA, based on two monoclonal antibodies, for quantification of fatty acid synthase. J Immunoassay Immunochem 2002;23:279–92.
18. Pizer E, Thupari J, Han W, et al. Malonyl-Coenzyme-A is a potential mediator of cytotoxicity induced by fatty-acid synthase inhibition in human breast cancer cells and xenografts. Cancer Res 2000;60:213–8.
19. Gabrielson EW, Pinn ML, Testa JR, Kuhajda FP. Increased fatty acid synthase is a therapeutic target in mesothelioma. Clin Cancer Res 2001;7:153–7.
20. Wang HQ, Altomare DA, Skele KL, et al. Positive feedback regulation between AKT activation and fatty acid synthase expression in ovarian carcinoma cells. Oncogene 2005;24:3574–82.
21. De Schrijver E, Brusselmans K, Heyns W, Verhoeven G, Swinnen JV. RNA interference-mediated silencing of the fatty acid synthase gene attenuates growth and induces morphological changes and apoptosis of LNCaP prostate cancer cells. Cancer Res 2003;63:3799–804.
22. Pizer E, Wood F, Heine H, Romantsey F, Pasternack G, Kuhajda F. Inhibition of fatty acid synthesis delays disease progression in a xenograft model of ovarian cancer. Cancer Res 1996;56:1189–93.
23. Kuhajda FP, Jenner K, Wood FD, et al. Fatty acid synthesis: a potential selective target for antineoplastic therapy. Proc Natl Acad Sci U S A 1994;91:6379–83.
24. Zhou W, Simpson PJ, McFadden JM, et al. Fatty acid synthase inhibition triggers apoptosis during S-phase in human cancer cells. Cancer Res 2003;63:7330–7.
25. Li JN, Gorospe M, Chrest FJ, et al. Pharmacological inhibition of fatty acid synthase activity produces both cytostatic and cytotoxic effects modulated by p53. Cancer Res 2001;61:1493–9.
26. Menendez JA, Lupu R. RNA interference-mediated silencing of the p53 tumor-suppressor protein drastically increases apoptosis after inhibition of endogenous fatty acid metabolism in breast cancer cells. Int J Mol Med 2005;15:33–40.
27. Menendez JA, Vellon L, Mehmi I, et al. Inhibition of fatty acid synthase (FAS) suppresses HER2/neu (erbB-2) oncogene overexpression in cancer cells. Proc Natl Acad Sci U S A 2004;101:10715–20.
28. Kumar-Sinha C, Ignatoski KW, Lippman ME, Ethier SP, Chinnaiyan AM. Transcriptome analysis of HER2 reveals a molecular connection to fatty acid synthesis. Cancer Res 2003;63:132–9.
29. Alli PM, Pinn ML, Jaffee EM, McFadden JM, Kuhajda FP. Fatty acid synthase inhibitors are chemopreventive for mammary cancer in neu-N transgenic mice. Oncogene 2005;24:39–46.
30. Kuhajda FP, Pizer EP, Li JL, Mani NS, Frehywot GL, Townsend CA. Synthesis and anti-tumor activity of a novel inhibitor of fatty acid synthase. Proc Natl Acad Sci U S A 2000;97:3450–4.
31. Loftus TM, Jaworsky DE, Frehywot GL, et al. Reduced food intake and body weight in mice treated with fatty acid synthase inhibitors. Science 2000;288:2379–81.
32. Thupari JN, Kim EK, Moran TH, Ronnett GV, Kuhajda FP. Chronic C75 treatment of diet-induced obese mice increases fat oxidation and reduces food intake to reduce adipose mass. Am J Physiol Endocrinol Metab 2004;287:E97–104.
33. Thupari JN, Landree LE, Ronnett GV, Kuhajda FP. C75 increases peripheral energy utilization and fatty acid oxidation in diet-induced obesity. Proc Natl Acad Sci U S A 2002;99:9488–502.
34. Nicot C, Napal L, Relat J, et al. C75 activates malonyl-CoA sensitive and insensitive components of the CPT system. Biochem Biophys Res Commun 2004;325:660–4.
35. Yang N, Kays JS, Skillman TR, Burris L, Seng TW, Hammond C. C75 activates carnitine palmitoyltransferase-1 in isolated mitochondria and intact cells without displacement of bound malonyl CoA. J Pharmacol Exp Ther 2005;312:127–33.
36. Landree LE, Hanlon AL, Strong DW, et al. C75, a fatty acid synthase inhibitor, modulates AMP-activated protein kinase to alter neuronal energy metabolism. J Biol Chem 2004;279:3817–27.
37. Kim EK, Miller I, Aja S, et al. C75, a fatty acid synthase inhibitor, reduces food intake via hypothalamic AMP-activated protein kinase. J Biol Chem 2004;279:19970–6.
38. Hardie DG, Carling D, Carlson M. The AMP-activated/SNF1 protein kinase subfamily: metabolic sensors of the eukaryotic cell? Annu Rev Biochem 1998;67:821–55.
39. Kemp BE, Mitchelhill KI, Stapleton D, Michell BJ, Chen ZP, Witters LA. Dealing with energy demand: the AMP-activated protein kinase. Trends Biochem Sci 1999;24:22–5.
40. McFadden JM, Medghalchi SM, Thupari JN, et al. Application of a flexible synthesis of (5*R*)-thiolactomycin to develop new inhibitors of type I fatty acid synthase. J Med Chem 2005;48:946–61.
41. Woods A, Cheung PC, Smith FC, et al. Characterization of AMP-activated protein kinase β and γ subunits. Assembly of the heterotrimeric complex *in vitro*. J Biol Chem 1996;271:10282–90.
42. Xing Y, Musi N, Fujii N, et al. Glucose metabolism and energy homeostasis in mouse hearts overexpressing dominant negative α2 subunit of AMP-activated protein kinase. J Biol Chem 2003;278:28372–7.
43. Smith S, Abraham S. Fatty acid synthase from lactating rat mammary gland. Methods Enzymol 1975;35:65–74.
44. Aprahamian SA, Arslanian MJ, Wakil SJ. Comparative studies on the kinetic parameters and product analyses of chicken and rat liver and yeast fatty acid synthetase. Comp Biochem Physiol B Biochem Mol Biol 1982;71:577–82.
45. Jayakumar A, Tai MH, Huang WY, et al. Human fatty acid synthase: properties and molecular cloning. Proc Natl Acad Sci U S A 1995;92:8695–9.
46. Watkins PA, Ferrell EV, Jr., Pedersen JI, Hoefler G. Peroxisomal fatty acid β-oxidation in HepG2 cells. Arch Biochem Biophys 1991;289:329–36.
47. Rubi B, Antinozzi PA, Herrero L, et al. Adenovirus-mediated overexpression of liver carnitine palmitoyltransferase I in INS1E cells: effects on cell metabolism and insulin secretion. Biochem J 2002;364:219–26.
48. Stocchi V, Cucchiarini L, Magnani M, Chiarantini L, Palma P, Crescentini G. Simultaneous extraction and reverse-phase high-performance liquid chromatographic determination of adenine and pyridine nucleotides in human red blood cells. Anal Biochem 1985;146:118–24.
49. Witters LA, Kemp BE. Insulin activation of acetyl-CoA carboxylase accompanied by inhibition of the 5′-AMP-activated protein kinase. J Biol Chem 1992;267:2864–7.
50. McFadden JM, Frehywot GL, Townsend CA. A flexible route to (5*R*)-thiolactomycin, a naturally occurring inhibitor of fatty acid synthesis. Org Lett 2002;4:3859–62.
51. Halvorson DL, McCune SA. Inhibition of fatty acid synthesis in isolated adipocytes by 5-(tetradecyloxy)-2-furoic acid. Lipids 1984;19:851–6.
52. Hardie DG, Hawley SA. AMP-activated protein kinase: the energy charge hypothesis revisited. BioEssays 2001;23:1112–9.
53. Woods A, Azzout-Marniche D, Foretz M, et al. Characterization of the role of AMP-activated protein kinase in the regulation of glucose-activated gene expression using constitutively active and dominant negative forms of the kinase. Mol Cell Biol 2000;20:6704–11.
54. Al-Khalili L, Chibalin AV, Yu M, et al. MEF2 activation in differentiated primary human skeletal muscle cultures requires coordinated involvement of parallel pathways. Am J Physiol Cell Physiol 2004;286:C1410–6.
55. Rattan R, Giri S, Singh AK, Singh I. 5-Amino-imidazole-4-carboxamide-1-β-4-ribofuranoside inhibits cancer cell proliferation *in vitro* and *in vivo* via AMP-activated protein kinase (AMPK). J Biol Chem 2005;280:39582–93.
56. Pizer E, Pflug B, Bova G, Han W, Udan M, Nelson J. Increased fatty acid synthase as a therapeutic target in androgen-independent prostate cancer progression. Prostate 2001;47:102–10.
57. Aja S, McFadden JM, Aplasca A, et al. Intracerebroventricular administration of either C89b, a stimulator of carnitinepalmitoyl-transferase-1 (CPT-1s), or cerulenin, an inhibitor of fatty acid synthase (FASi), reduces food intake and body weight in mice. Appetite 2006;46:339.
58. Hardie DG, Carling D. The AMP-activated protein kinase-fuel gauge of the mammalian cell? Eur J Biochem 1997;246:259–73.
59. Abbud W, Habinowski S, Zhang JZ, et al. Stimulation of AMP-activated protein kinase (AMPK) is associated with enhancement of Glut1-mediated glucose transport. Arch Biochem Biophys 2000;380:347–52.
60. Kurth-Kraczek EJ, Hirshman MF, Goodyear LJ, Winder WW. 5′ AMP-activated protein kinase activation causes GLUT4 translocation in skeletal muscle. Diabetes 1999;48:1667–71.
61. Marsin AS, Bertrand L, Rider MH, et al. Phosphorylation and activation of heart PFK-2 by AMPK has a role in the stimulation of glycolysis during ischaemia. Curr Biol 2000;10:1247–55.
62. Winder WW, Hardie DG. Inactivation of acetyl-CoA carboxylase and activation of AMP-activated protein kinase in muscle during exercise. Am J Physiol 1996;270:E299–304.
63. Motoshima H, Goldstein BJ, Igata M, Araki E. AMPK and cell proliferation-AMPK as a therapeutic target for atherosclerosis and cancer. J Physiol 2006;574:63–71.
64. Xiang X, Saha AK, Wen R, Ruderman NB, Luo Z. AMP-activated protein kinase activators can inhibit the growth of prostate cancer cells by multiple mechanisms. Biochem Biophys Res Commun 2004;321:161–7.
65. Imamura K, Ogura T, Kishimoto A, Kaminishi M, Esumi H. Cell cycle regulation via p53 phosphorylation by a 5′-AMP activated protein kinase activator, 5-aminoimidazole-4-carboxamide-1-β-D-ribofuranoside, in a human hepatocellular carcinoma cell line. Biochem Biophys Res Commun 2001;287:562–7.
66. Igata M, Motoshima H, Tsuruzoe K, et al. Adenosine monophosphate-activated protein kinase suppresses vascular smooth muscle cell proliferation through the inhibition of cell cycle progression. Circ Res 2005;97:837–44.
67. Ruderman NB, Saha AK, Kraegen EW. Minireview: malonyl CoA, AMP-activated protein kinase, and adiposity. Endocrinology 2003;144:5166–71.
68. Funabashi H, Kawaguchi A, Tomoda H, Omura S, Okuda S, Iwasaki S. Binding site of cerulenin in fatty acid synthetase. J Biochem (Tokyo) 1989;105:751–5.
69. Weiss L, Hoffmann GE, Schreiber R, et al. Fatty-acid biosynthesis in man, a pathway of minor importance. Purification, optimal assay conditions, and organ distribution of fatty-acid synthase. Biol Chem Hoppe Seyler 1986;367:905–12.